Available online at www.sciencedirect.com
SCIENCE DIRECT®
International Journal of Heat and Mass Transfer 48 (2005) 1186–1194
International Journal of HEAT and MASS TRANSFER
www.elsevier.com/locate/ijhmt

Swelling controlled release of drug in spherical polymer-penetrant systems

Jenn-Sen Lin *, Yu-Lin Peng

Department of Mechanical Engineering, National United University, Miao-Li 360, Taiwan, ROC

Received 24 April 2003; received in revised form 5 March 2004
Available online 8 December 2004

Abstract

The study addresses problems of moving boundaries that involve mass diffusion in a spherical swelling polymer-penetrant system with a controlled release of drug. The method of perturbation is applied and the complete time history of the penetrant front and the volume expansion front are determined for small control values of ε; the local similarity method is used to expand the results for large ε. The results reveal that the velocity of penetrant and the release rate of the drug near $t^* = 0$ are constant, regardless of the diameter of the sphere. The velocity and rate decrease over a short period, and then increase again as the penetrant front proceeds to the sphere center. If ε and $\bar{v}$ are small, the volume expansion front is almost unchanged and only the time history of the penetrant front in the swelling polymer-penetrant system needs to be considered.

Keywords: Moving boundaries; Local similarity method; Polymer; Controlled release

1. Introduction

When a glassy polymer is exposed to a penetrant solvent, which can be gas or liquid, the solvent diffuses into the polymer to form a glassy–rubbery interface that moves through the polymer. In 1966, Alfrey et al. [1] indicated that in polymer-penetrant systems, the motion of the penetrant front is a function of time that differs significantly from the classical function of $t^{1/2}$ associated with Fickian relaxation. Various theories or equations of motion are needed to describe accurately the diffusion in individual polymer-penetrant system, according to the type of polymer, the type of penetrant and the ambient conditions.

For some polymer-penetrant systems, however, relatively slow molecular relaxation occurs only at or near the glass/rubber interface, while instantaneous Fickian diffusions occur in both glassy and rubbery regions. In such systems, a local driving force, associated with differences between concentrations of the solvent, dominates the motion of the interface. Astarita and Sarti [2], and Andreucci and Ricci [3] developed mathematical models of the sorption of swelling solvents in glassy polymers and considered the kinetics and driving force of swelling. Cohen [4,5] analyzed problems related to diffusion in glassy polymers and employed an integral approximation to study the motions of the penetrant front and glass-gel interface. Cohen and Erneux [6]

* Corresponding author. Tel.: +886 37381321; fax: +886 37381333.
E-mail address: jsenlin@nuu.edu.tw (J.-S. Lin).

0017-9310/$ - see front matter © 2004 Elsevier Ltd. All rights reserved.
doi:10.1016/j.ijheatmasstransfer.2004.08.031

Nomenclature

$A(t^*)$	arbitrary function of t^* in Eq. (35)	r_i	initial penetrant front and volume expansion front
$A^*(t^*)$	arbitrary function of t^* in Eq. (41)	r_i^*	initial dimensionless penetrant front and volume expansion front
$B(r,t)$	drug concentration	R_i	penetrant front
B_0	constant concentration of drug	R_i^*	dimensionless penetrant front
$C(r,t)$	solvent concentration	R_f	volume expansion front
C_0	solubility of the solvent in the swollen polymer	R_f^*	dimensionless volume expansion front
C^*	threshold solvent concentration	$\widetilde{R}_i^*$	R_i^*/r_i^*
$\overline{C}$	$C^* + K$	$\widetilde{R}_f^*$	R_f^*/r_i^*
D	diffusion coefficient of the solvent	t	time
D_d	diffusion coefficient of the drug	t^*	dimensionless time
k_1, k_2	phenomenological quantities	u	dimensionless solvent concentration
K	k_2/k_1	v	dimensionless drug concentration
m	drug release rate	$\bar{v}$	molar volume of the swelling agent
n	phenomenological quantity	$X(t^*)$	constant function of t^* in Eq. (45)
r	penetrant front and volume expansion front	$X^*(t^*)$	constant function of t^* in Eq. (46)
r^*	dimensionless penetrant front and volume expansion front	ε	control parameter

considered the diffusive behavior of the penetrant front through the polymer under the limiting conditions that the time is approximately zero or infinity; they completed the time evolution of the penetrant front using perturbation technique with a small control parameter. In so-called ''case II diffusion'', sharp concentration fronts often move with constant speed [7,8]. Guidotti [9] and Guidotti and Pelesko [10] studied the transient instability and free boundary conditions in case II diffusion. Higuchi [11,12] formulated models of the release rate of a solid drug by diffusion through a polymer, obtaining results for planar surfaces and spherical pellets. Peppas et al. [13] considered drug initially uniformly distributed in a polymeric matrix and determined the drug concentration profile within the polymer and drug release rates due to swelling. Lin et al. [14] further considered the swelling controlled release of a drug and solvent transport systems. They simulated these processes using a local similarity algorithm. The transport phenomenon in a spherical polymer-penetrant system has been studied with reference to inward diffusion [15], but without considering the volume expansion front.

This study considers the simultaneous swelling controlled release in a spherical polymer matrix of a dissolved drug and the swelling solvent. Accordingly, the volume expansion of the polymer enables, both a glassy–rubbery interface and a moving boundary to be formed at two locations. The perturbation method and a numerical treatment of local similarities are employed to investigate the complete time history of these boundaries with various parameters.

2. Mathematical model of spherical polymer-penetrant system

This work investigates the diffusion of a drug in a swollen polymer, when the drug is added to a penetrant solvent. The drug is considered to be dissolved within the polymer matrix but not able to diffuse through the matrix. When the penetrant solvent starts to diffuse into the polymer, the drug simultaneously begins to diffuse through the swollen part of the polymer. Hence, the release rate of the drug is determined by the rate of diffusion of the solvent in the polymer. The volume expansion of the swollen polymer is considered to enable the movement of both the polymer surface and the penetrant front throughout the matrix. Fig. 1 shows the physical concentration profiles of the drug (full line) and the solvent (dash line) problem in the spherical system. B and C represent the drug concentration and solvent concentration, respectively. The diffusivity D of the swollen polymer is taken to be constant. C_0 is the solubility of the solvent in the swollen polymer. B_0 is the constant concentration of the drug which is initially loaded and maintained in the solvent-free matrix. Fig. 1 includes two moving fronts. One at $r = R_i(t)$ separates the solvent-free polymer from the swollen polymer. The other at $r = R_f(t)$ is associated with the volume expansion of the polymer due to its gradual swelling. The polymer surface is initially located at $R_i(0) = R_f(0) = r_i$. The diffusions of the drug and solvent are formulated as a one-dimensional spherical moving boundary problem for the concentration $B(r,t)$ of the drug, the

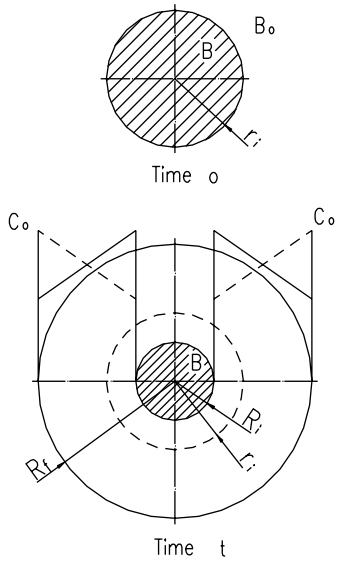

Fig. 1. Physical configuration of the spherical swelling-controlled release system.

concentration $C(r,t)$ of the penetrant, and the position $r(t)$ of the interface:

$$\frac{\partial C}{\partial t} = D\left(\frac{1}{r}\frac{\partial^2(rC)}{\partial r^2}\right) \qquad R_i(t) < r < R_f(t) \tag{1}$$

$$C = C_0 > C^* \qquad \text{at } r = R_f(t) \tag{2}$$

$$(C+K)\frac{dR_i}{dt} = -D\frac{\partial C}{\partial r} \qquad \text{at } r = R_i(t) \tag{3}$$

$$\frac{dR_i}{dt} = -k_1(C-C^*)^n \qquad \text{at } r = R_i(t) \tag{4}$$

$$\frac{\partial B}{\partial t} = D_d\left(\frac{1}{r}\frac{\partial^2(rB)}{\partial r^2}\right) \qquad R_i(t) < r < R_f(t) \tag{5}$$

$$B = 0 \qquad \text{at } r = R_f(t) \tag{6}$$

$$(B-B_0)\frac{dR_i}{dt} = -D_d\frac{\partial B}{\partial r} \qquad \text{at } r = R_i(t) \tag{7}$$

$$R_f^3(t) - r_i^3 = 3\bar{v}\int_{R_i(t)}^{R_f(t)} C(r,t)r^2 dr \tag{8}$$

$$R_i(0) = R_f(0) = r_i, \tag{9}$$

where k_1, K, D, C^*, and C_0 are constant parameters. The first four are material parameters; the latter is the system parameter. The parameters K, k_1, and n are phenomenological quantities, which can be obtained experimentally. Eq. (1) represents Fick's law for a one-dimensional system and Eq. (2) describes the associated boundary condition at the surface. Eq. (4) represents the local kinetics that drives the penetrant front at some finite rate. Eq. (3) states the mass balance at the moving interface. The flux across a moving boundary of the swelling region is given by $-D\partial C/\partial r - C dR_i/dt$ and is assumed to be proportional to the flux generated by the interface region. Hence, we have

$$-D\frac{\partial C}{\partial r} - C\frac{dR_i}{dt} = k_2(C-C^*)^n \qquad \text{at } r = R_i(t) \tag{10}$$

Substituting Eq. (10) into Eq. (4) yields Eq. (3), wherein $K = k_2/k_1$. D and D_d are dimensional diffusion coefficients of the solvent and drug, respectively. Eqs. (5)–(7) represent the diffusion of the drug in the swollen polymer. The volume change of the polymer due to gradual swelling and the initial condition are expressed by Eqs. (8) and (9), respectively, where $\bar{v}$ is the molar volume of the swelling agent.

Eqs. (1)–(9) can be rendered dimensionless using the following dimensionless variables:

$$t^* = \frac{t}{\alpha} \qquad u = \frac{C-C^*}{C_0-C^*} \qquad v = \frac{B}{B_0} \qquad r^* = \frac{r}{\beta}$$

$$r_i^* = \frac{r_i}{\beta} \qquad R_i^* = \frac{R_i}{\beta} \qquad R_f^* = \frac{R_f}{\beta} \tag{11}$$

$$\alpha = \frac{D(C_0-C^*)^{1-2n}}{\overline{C}k_1^2} \qquad \beta = \frac{D(C_0-C^*)^{1-n}}{\overline{C}k_1}$$

$$\overline{C} = C^* + K$$

The following equation hold.

$$\frac{\partial u}{\partial t^*} = \frac{1}{\varepsilon}\left(\frac{1}{r^*}\frac{\partial^2(r^*u)}{\partial r^{*2}}\right) \qquad R_i^*(t^*) < r^* < R_f^*(t^*) \tag{12}$$

$$u = 1 \qquad \text{at } r^* = R_f^*(t^*) \tag{13}$$

$$(1+\varepsilon u)\frac{dR_i^*}{dt^*} = -\frac{\partial u}{\partial r^*} \qquad \text{at } r^* = R_i^*(t^*) \tag{14}$$

$$\frac{dR_i^*}{dt^*} = -u^n \qquad \text{at } r^* = R_i^*(t^*) \tag{15}$$

$$\frac{\partial v}{\partial t^*} = \frac{D_d}{D}\frac{1}{\varepsilon}\left(\frac{1}{r^*}\frac{\partial^2(r^*v)}{\partial r^{*2}}\right) \qquad R_i^*(t^*) < r^* < R_f^*(t^*) \tag{16}$$

$$v = 0 \qquad \text{at } r^* = R_f^*(t^*) \tag{17}$$

$$\varepsilon(v-1)\frac{dR_i^*}{dt^*} = -\frac{D_d}{D}\frac{\partial v}{\partial r^*} \qquad \text{at } r^* = R_i^*(t^*) \tag{18}$$

$$R_f^{*3}(t^*) - r_i^{*3} = 3\bar{v}\overline{C}^2\int_{R_i^*(t^*)}^{R_f^*(t^*)}\left(\frac{C^*}{\overline{C}} + \varepsilon u\right)^2 dr^* \tag{19}$$

$$R_i^*(0) = R_f^*(0) = r_i^* \tag{20}$$

where ε is a control parameter defined as

$$\varepsilon = \frac{C_0 - C^*}{\overline{C}} \tag{21}$$

The parameter C^* is the threshold concentration for swelling and, therefore, the parameter ε must be greater than zero to ensure movement of the interface.

3. Perturbation method

Solving the moving boundary problem analytically is very difficult. Therefore, an asymptotic solution to the system is considered. In this section, the perturbation method is used to describe the complete time history of the penetrant and the volume expansion fronts as the limit ε approaches zero. The asymptotic solution to these equations is assumed to be

$$u(r^*, t^*, \varepsilon) = u_0(r^*, t^*) + \varepsilon u_1(r^*, t^*) + \cdots \tag{22}$$

$$v(r^*, t^*, \varepsilon) = v_0(r^*, t^*) + \varepsilon v_1(r^*, t^*) + \cdots \tag{23}$$

$$R_{\mathrm{i}}^*(t^*, \varepsilon) = R_{\mathrm{i}0}^*(t^*) + \varepsilon R_{i1}^*(t^*) + \cdots \tag{24}$$

$$R_{\mathrm{f}}^*(t^*, \varepsilon) = R_{\mathrm{f}0}^*(t^*) + \varepsilon R_{\mathrm{f}1}^*(t^*) + \cdots \tag{25}$$

Substituting Eqs. (22)–(25) into Eqs. (12)–(20) and equating to zero the coefficients of each power of ε yields the following equations for u_0 and v_0:

$$\left(\frac{1}{r^*}\frac{\partial^2(r^* u_0)}{\partial r^{*2}}\right) = 0 \qquad R_{\mathrm{i}0}^*(t^*) < r^* < R_{\mathrm{f}0}^*(t^*) \tag{26}$$

$$u_0 = 1 \qquad \text{at } r^* = R_{\mathrm{f}0}^*(t^*) \tag{27}$$

$$\frac{\mathrm{d}R_{\mathrm{i}0}^*}{\mathrm{d}t^*} = -\frac{\partial u_0}{\partial r^*} \qquad \text{at } r^* = R_{\mathrm{i}0}^*(t^*) \tag{28}$$

$$\frac{\mathrm{d}R_{\mathrm{i}0}^*}{\mathrm{d}t^*} = -u_0^n \qquad \text{at } r^* = R_{\mathrm{i}0}^*(t^*) \tag{29}$$

$$\left(\frac{1}{r^*}\frac{\partial^2(r^* v_0)}{\partial r^{*2}}\right) = 0 \qquad R_{\mathrm{i}0}^*(t^*) < r^* < R_{\mathrm{f}0}^*(t^*) \tag{30}$$

$$v_0 = 0 \qquad \text{at } r^* = R_{\mathrm{f}0}^*(t^*) \tag{31}$$

$$\frac{\partial v_0}{\partial r^*} = 0 \qquad \text{at } r^* = R_{\mathrm{i}0}^*(t^*) \tag{32}$$

$$R_{\mathrm{f}0}^{*3}(t^*) - r_{\mathrm{i}}^{*3} = 3\bar{v}C^{*^2}(R_{\mathrm{f}0}^* - R_{\mathrm{i}0}^*) \tag{33}$$

$$R_{\mathrm{i}0}^*(0) = R_{\mathrm{f}0}^*(0) = r_{\mathrm{i}}^* \tag{34}$$

The solutions to Eq. (26) with boundary condition (27) is

$$u_0(r^*, t^*) = 1 + A(t^*)\left(\frac{1}{r^*} - \frac{1}{R_{\mathrm{f}0}^*}\right) \tag{35}$$

where $A(t^*)$ is an arbitrary functions of t^* determined by Eqs. (28), (29), and (34). Substituting Eq. (35) into Eqs. (28) and (29) enables $A(t^*)$ to be eliminated and the following ordinary differential equation obtained for $R_{\mathrm{i}0}$ and $R_{\mathrm{f}0}$;

$$\frac{\mathrm{d}R_{\mathrm{i}0}^*}{\mathrm{d}t^*} = -\left[1 + R_{\mathrm{i}0}^{*2}\frac{\mathrm{d}R_{\mathrm{i}0}^*}{\mathrm{d}t^*}\left(\frac{1}{R_{\mathrm{i}0}^*} - \frac{1}{R_{\mathrm{f}0}^*}\right)\right]^n \tag{36}$$

If $n = 1$, integrating Eq. (36) yields

$$R_{\mathrm{i}0}^* - R_{\mathrm{f}0}^* + \frac{1}{2}(R_{\mathrm{i}0}^{*2} - R_{\mathrm{f}0}^{*2}) - \frac{1}{3R_{\mathrm{f}0}^*}(R_{\mathrm{i}0}^{*3} - R_{\mathrm{f}0}^{*3}) = -t^* \tag{37}$$

If ε is sufficiently small, then the positions of the penetrant front and the volume expansion front over a long period are given by Eqs. (33) and (37) using Newton–Raphson iteration with initial conditions $R_{\mathrm{i}0}^*(0) = R_{\mathrm{f}0}^*(0) = r_{\mathrm{i}}^*$. If the radius of sphere is large enough, the interface moves through the polymer at a constant velocity for small times. Thus, the position of interface is proportional to t^* (i.e. $R_{\mathrm{f}0}^* - R_{\mathrm{i}0}^* = t^*$), in a manner consistent with a planar system [6].

Next, the problem with $v_1(r^*,t^*)$, which is described as follows (since $v_0 = 0$, obtained from Eqs. (30)–(32)), is considered.

$$\left(\frac{1}{r^*}\frac{\partial^2(r^* v_1)}{\partial r^{*2}}\right) = 0 \qquad R_{\mathrm{i}0}^*(t^*) < r^* < R_{\mathrm{f}0}^*(t^*) \tag{38}$$

$$v_1 = 0 \qquad \text{at } r^* = R_{\mathrm{f}0}^*(t^*) \tag{39}$$

$$\frac{\mathrm{d}R_{\mathrm{i}0}^*}{\mathrm{d}t^*} = \frac{D_{\mathrm{d}}}{D}\frac{\partial v_1}{\partial r^*} \qquad \text{at } r^* = R_{\mathrm{i}0}^*(t^*) \tag{40}$$

From Eqs. (38) and (39),

$$v_1(r^*, t^*) = A^*(t^*)\left(\frac{1}{r^*} - \frac{1}{R_{\mathrm{f}0}^*}\right) \tag{41}$$

where $A^*(t^*)$ is an arbitrary function of t^* determined by Eq. (40).

$$A^*(t^*) = -\frac{D}{D_{\mathrm{d}}}R_{\mathrm{i}0}^{*2}\frac{\mathrm{d}R_{\mathrm{i}0}^*}{\mathrm{d}t^*} \tag{42}$$

Substituting Eq. (42) into Eq. (41) yields, the concentration of the drug

$$v(r^*, t^*) = -\varepsilon\frac{D}{D_{\mathrm{d}}}\left(\frac{1}{r^*} - \frac{1}{R_{\mathrm{f}}^*}\right)R_{\mathrm{i}}^{*2}\frac{\mathrm{d}R_{\mathrm{i}}^*}{\mathrm{d}t^*} \tag{43}$$

The asymptotic solution for the drug release rate at small times is

$$m = \left[-\frac{\partial v}{\partial r^*}\right]_{r^* = R_{\mathrm{i}}^*} = -\varepsilon\frac{D}{D_{\mathrm{d}}}\left(\frac{R_{\mathrm{i}}^*}{R_{\mathrm{f}}^*}\right)^2\frac{\mathrm{d}R_{\mathrm{i}}^*}{\mathrm{d}t^*} \tag{44}$$

The drug release rate thus depends on the control parameter ε, the radius of sphere, the diffusion coefficients of the solvent and drug, and the velocity of penetrant.

4. Method of similarity solution

This section proposes a method for numerically solving the moving boundary problem (Eqs. (12)–(20)). A local similarity solution can be applied to the spherical polymer-penetrant system as follows;

$$u(r^*,t^*)=\frac{X(t^*)}{r^*}\operatorname{erf}\left(\frac{R_{\mathrm{f}}^*-r^*}{2\sqrt{\varepsilon^{-1}t^*}}\right)+\frac{R_{\mathrm{f}}^*}{r^*} \tag{45}$$

and

$$v(r^*,t^*)=\frac{X^*(t^*)}{r^*}\operatorname{erf}\left(\frac{R_{\mathrm{f}}^*-r^*}{2\sqrt{\varepsilon^{-1}t^*D_{\mathrm{d}}/D}}\right) \tag{46}$$

which equations automatically satisfy the boundary conditions (13) and (17), respectively. Eqs. (45) and (46) are exact solutions to diffusion equations (12) and (16), respectively, only if X and X^* are constants. However, the parameters X and X^* satisfied the boundary conditions are not constants herein. A numerical technique can be used to obtain the penetrant and volume expansion fronts in which X and X^* are piece-wise constants during an interval $(t_{i-1}^*, t_{\mathrm{i}}^*)$. t_{i-1}^* and t_{i}^* represent the $(i-1)$th and ith specified times. The small interval is chosen to reduce the errors result from the numerical calculation. In the numerical simulation, the diffusion coefficients D and D_{d} are equal under the specified conditions $C^* = 0.08$ and $k_2/k_1 = 1$.

The procedure for numerical calculation is as follows.

(a) Locate of the initial penetrant front and volume expansion front at $R_{\mathrm{i}}^*(0) = R_{\mathrm{f}}^*(0) = r_{\mathrm{i}}^*$ and set the initial velocity $\mathrm{d}R_{\mathrm{i}}^*(0)/\mathrm{d}t^* = -1$.
(b) Substitute Eqs. (45) and (15) into Eq. (14) to obtain a nonlinear equation for X which is solved by Newton–Raphson iteration.
(c) Integrate the position of the penetrant front, R_{i}^* obtained from Eq. (15) using Runge–Kutta integration after determining X.
(d) Substitute Eq. (46) into Eq. (18) to calculate the values of X^* and the drug release rate m.
(e) Calculate the position of the volume expansion front from Eq. (19).
(f) Obtain the diffusion region between the penetrant and the volume expansion boundaries in the subsequent time step.

Repeating steps (b) to (f) yields the complete time history of the penetrant and volume expansion fronts.

5. Results and discussion

The time step in the numerical simulations must be appropriately chosen to ensure accuracy. Shorting the time step increases accuracy, but also increases computing time. A smaller time step should be used for simulation for short times because of the penetrant has a high velocity, while larger time step can be used in simulating a long-term behavior. Fig. 2 shows the effect of the time step on the constant X. The efficient computational procedures involve the time steps 0.001 for $t^* < 0.5$ and 0.01 for $t^* \geqslant 0.5$. Fig. 3 presents the computated constant $X(t^*)$ for various control parameters ε.

From Fig. 4, when the radius of sphere is large enough, the numerical results approach those of a planar system, as studied by Cohen and Erneux [6]. Fig. 5 compares the numerical simulations with the asymptotic solutions with various ε. Both the asymptotic solutions, described in Section 3, and the numerical results for the positions of the penetrant front are almost the same

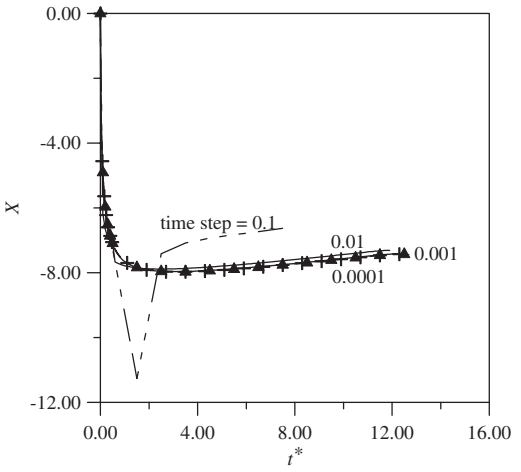

Fig. 2. X for various time steps ($\varepsilon = 1$, $\bar{v} = 1$, $n = 1$, $r_{\mathrm{i}}^* = 5$). (—) time step=0.01, (▲) time step=0.001, (+) time step = 0.0001.

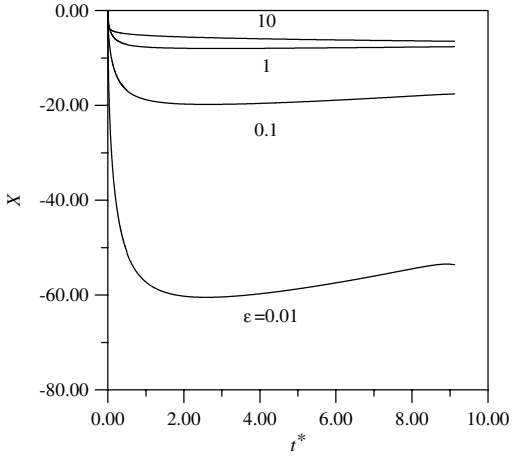

Fig. 3. X for each time step for different ε ($n = 1$, $r_{\mathrm{i}}^* = 5$).

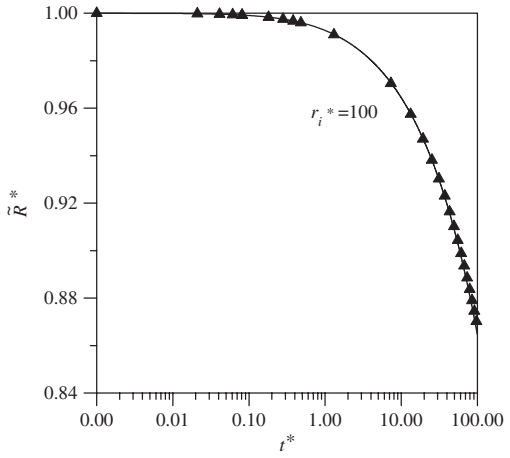

Fig. 4. Complete time histories of the positions of the penetrant front $\tilde{R}^*$ with $r_i^* = 100$ ($n = 1$, $\varepsilon = 0.1$, $\bar{v} = 1$). (▲) obtained from Cohen and Erneux [6].

when ε is very small. However, the asymptotic method cannot describe the time history behavior for large values of ε.

Fig. 6 displays the complete time histories of the penetrant front and the volume expansion front for $n = 1$ and $r_i^* = 5$ under different ε and $\bar{v}$. According to this figure, the small ε leads the penetrant front to reach quickly the center of sphere while the volume expansion front remain almost unchanged, as revealed in Table 1. Figs. 6 and 7 show the effect of parameters $\bar{v}$ on the penetrant and volume expansion fronts is shown in. The effect of the small parameter $\bar{v}$ on the volume expansion front

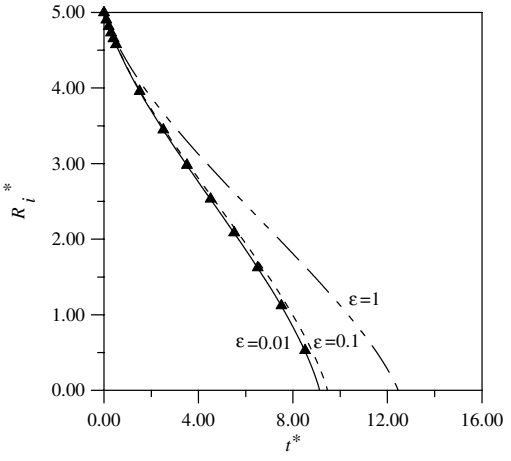

Fig. 5. Complete time histories of the position of the penetrant front R_i^* with different ε ($n = 1$, $\bar{v} = 0.1$, $r_i^* = 5$). (▲) asymptotic solutions from Eqs. (33) and (36) by the Newton–Raphson method.

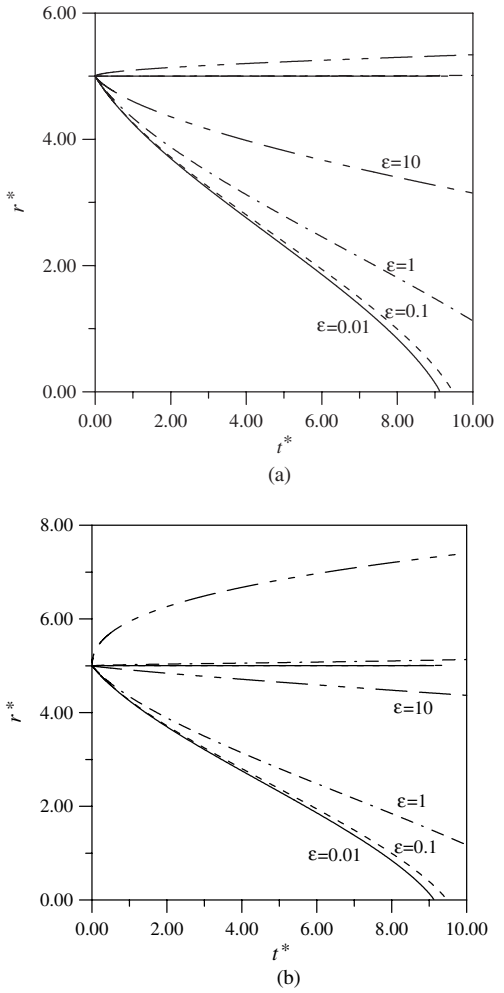

Fig. 6. Complete time histories of the positions of the penetrant front, R_i^*, and the volume expansion front, R_f^*, for different ε; (a) $\bar{v} = 0.1$ (b) $\bar{v} = 1$ for $n = 1$ and $r_i^* = 5$. The lower and upper lines represent R_i^* and R_f^*, respectively.

is similar to the effect of the small parameter ε on this front. Hence, the movement of the volume expansion front can be ignored at small ε and $\bar{v}$.

Figs. 8 and 9 depict the complete time histories of the penetrant front and volume expansion front, respectively. When r_i^*, which specifies the initial position, is large enough, the volume expansion front swells outward quite slowly. Thus, the effect of large r_i^* on the volume expansion front is negligible and only its effect on the penetrant front needs to be discussed. These results differ from those for a planar system [6,14], as they were based on the assumption that the semi-infinite swelling-control release drug system to be of unit thickness. Therefore, the volume expansion front in the planar system moves outwardly more quickly than that in an spherical system.

Table 1
Comparisons of the time histories of positions of volume expansion front, specified by R_f^*, for various parameters ε ($n = 1$, $\bar{v} = 0.1$, $r_i^* = 5$)

Time t^*	Asymptotic solution	Numerical solution		
		$\varepsilon = 0.01$	$\varepsilon = 0.1$	$\varepsilon = 1$
0.0	5.0000000	5.0000000	5.0000000	5.0000000
0.5	5.0000107	5.0000136	5.0000502	5.0014360
1.0	5.0000192	5.0000238	5.0000838	5.0022411
1.5	5.0000265	5.0000328	5.0001123	5.0029000
2.0	5.0000333	5.0000409	5.0001383	5.0034932
2.5	5.0000396	5.0000486	5.0001632	5.0040517
3.0	5.0000457	5.0000560	5.0001874	5.0045914
3.5	5.0000516	5.0000632	5.0002116	5.0051218
4.0	5.0000573	5.0000703	5.0002360	5.0056500
4.5	5.0000631	5.0000774	5.0002610	5.0061811
5.0	5.0000687	5.0000845	5.0002869	5.0067196
5.5	5.0000745	5.0000918	5.0003140	5.0072697
6.0	5.0000803	5.0000993	5.0003428	5.0078354
6.5	5.0000863	5.0001071	5.0003739	5.0084211
7.0	5.0000925	5.0001154	5.0004079	5.0090315
7.5	5.0000991	5.0001243	5.0004462	5.0096720
8.0	5.0001063	5.0001342	5.0004903	5.0103491
8.5	5.0001143	5.0001458	5.0005433	5.0110707
9.0	5.0001240	5.0001603	5.0006110	5.0118472

The asymptotic solution is calculated from Eqs. (33) and (36) by the Newton–Raphson method.

When $n = 0$ and Eq. (29) or Eq. (36) is integrated, the difference between the positions of the volume expansion and the penetrant fronts of the spherical system is equal to t^* ($R_{f0}^* - R_{i0}^* = t^*$) at all times. If $n = 1$, ε is small, and the radius of sphere is large, then the interfacial difference between the positions of the volume expansion and penetrant fronts over a long period is proportional to t^* ($R_{f0}^* - R_{i0}^* = t^*$). These results are consistent with those for a planar system [6]. Figs. 10 and 11 represent the penetrant and volume expansion fronts for three different values of n.

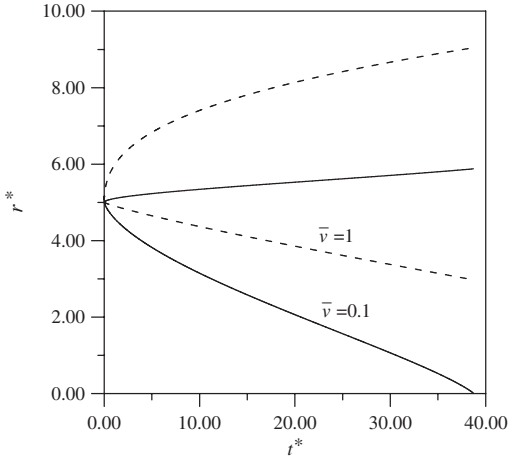

Fig. 7. Complete time histories of the positions of the penetrant front, R_i^*, and the volume expansion front, R_f^*, for different $\bar{v}$ ($n = 1$, $\varepsilon = 10$, $r_i^* = 5$). The lower and upper lines represent R_i^* and R_f^*, respectively.

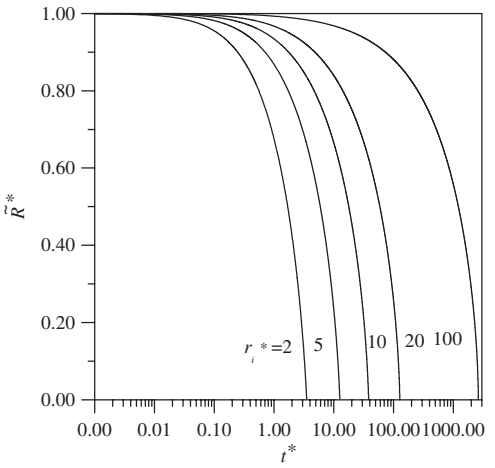

Fig. 8. Complete time histories of the positions of the penetrant front $\tilde{R}^*$ with different r_i^* ($n = 1$, $\varepsilon = 1$, $\bar{v} = 1$).

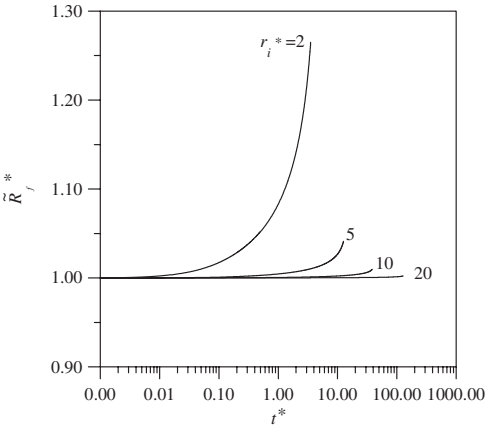

Fig. 9. Complete time histories of the positions of the volume expansion front R_f^* with different r_i^* ($n = 1$, $\varepsilon = 1$, $\bar{v} = 1$).

Fig. 12 displays the time history of the penetrant velocity for various ε. This figure indicates that increasing the control parameter ε decreases the penetrant velocity. It also indicates that the velocity of the volume expansion front increases with ε (as observed in Fig. 6). As ε approaches zero, the inward penetrant velocity remains constant over a longer period. Hence, the penetrant front take more time to reach the center of sphere when ε is large. The penetrant velocity decreases with time. However, the penetrant velocity increases

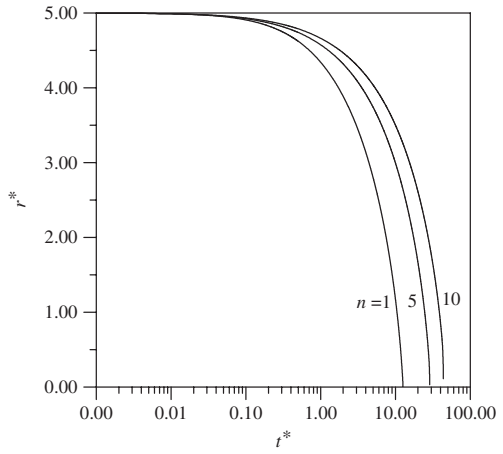

Fig. 10. Complete time histories of the positions of the penetrant front r^* with different n ($r_i^* = 5$, $\varepsilon = 1$, $\bar{v} = 1$).

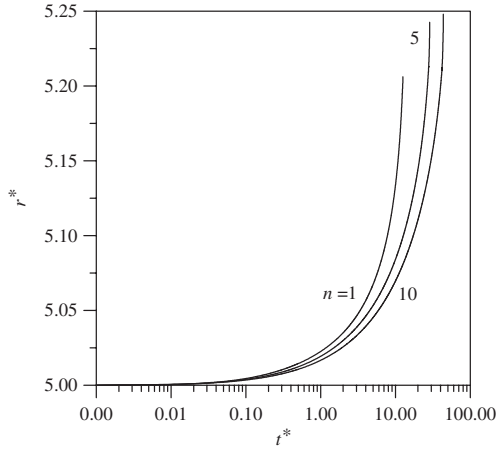

Fig. 11. Complete time histories of the positions of the volume expansion front R_f^* with different n ($r_i^* = 5$, $\varepsilon = 1$, $\bar{v} = 1$).

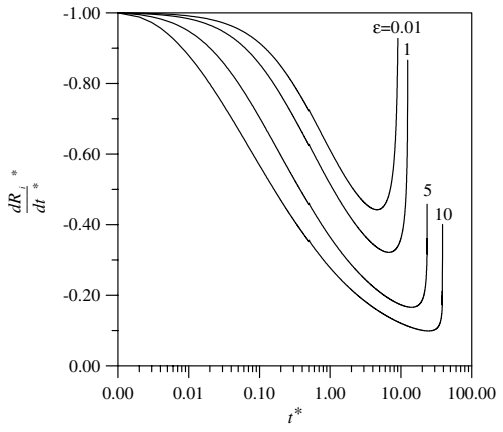

Fig. 12. Complete time histories of the velocities of the penetrant front R_i^* with different ε ($n = 1$, $\bar{v} = 1$, $r_i^* = 5$).

again as the penetrant front approaches the center of sphere.

From Eq. (44), the asymptotic drug release rate depends on the control parameter ε, radius of sphere, the diffusion coefficients of the solvent and drug and the penetrant velocity of the polymer front. Fig. 13 compares the numerical solutions with the asymptotic solutions for the drug release rate. When ε is very small, these two solutions are consistent with each other over short periods. The drug release rate remains constant over short periods. However, the asymptotic solution is no longer useful for describing the behavior of the drug release rate for large values of ε over long periods. A comparison between Figs. 12 and 13 shows that the

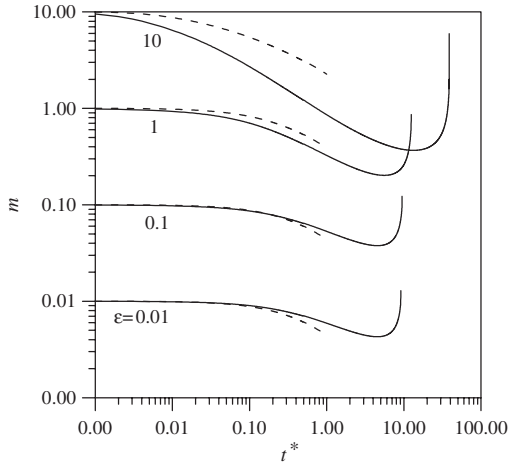

Fig. 13. Complete time histories of the drug release rates with different ε ($n = 1$, $\bar{v} = 0.1$, $r_i^* = 5$). Dash lines are calculated from Eq. (43).

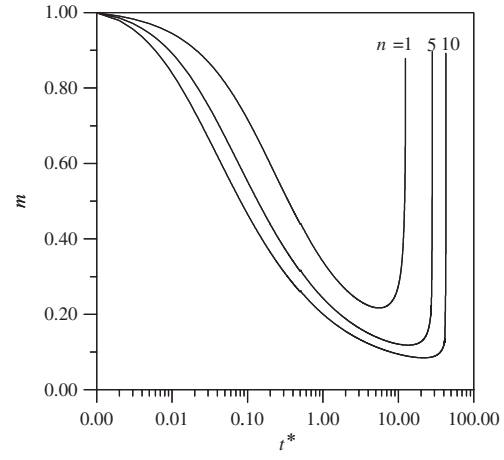

Fig. 14. Complete time histories of the drug release rates with different n ($\varepsilon = 1$, $\bar{v} = 0.1$, $r_i^* = 5$).

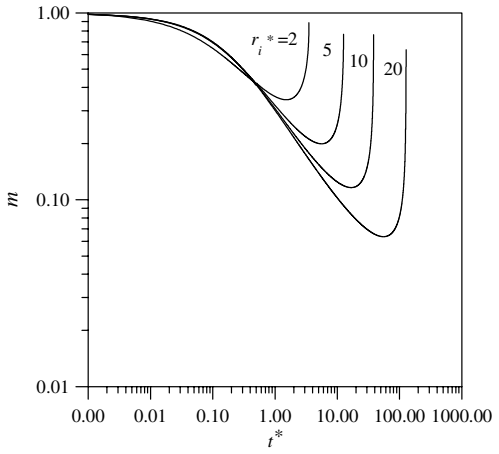

Fig. 15. Complete time histories of the drug release rates with different r_i^* ($n = 1$, $\varepsilon = 1$, $\bar{v} = 0.1$).

drug release rate is similar to the penetrant velocity, implying that the drug release rate is a function of the penetrant velocity and ε. The rate of the release of the drug increases as the penetrant front approaches the center of sphere. Figs. 14 and 15 show the effects of the parameters n and r_i^* on the drug release rate.

6. Conclusion

This work proposes a local similarity method and asymptotic method to simulate a free boundary problem that involves swelling-controlled release pharmaceuticals. This investigation has presented relevant analyses theoretical investigations have been presented in this study. The findings are summarized as follows:

(1) If the radius of the sphere is large enough, then the numerical results approach the solutions for a planar system, as studied by Cohen and Erneux [6].
(2) Numerical solutions are useful for all ε, whereas asymptotic solutions are valid only for small ε.
(3) If the radius of sphere is sufficiently large and small ε and $\bar{v}$ are adopted, then the position of the volume expansion front remains almost unchanged. If volume expansion effect is ignored, then the system reduces to a one-way diffusion problem.
(4) The asymptotic drug release rate depends on the control parameter, diffusion coefficients and the velocity of penetrant. The drug release rate at all times follows the velocity of the penetrant. The penetrant velocity and the drug release rate increase as the penetrant front penetrates closer to the center of the sphere.

Acknowledgments

The authors would like to thank the National Science Council of the Republic of China for supporting this research under Grant Number NSC-91-2212-E-239-006.

References

[1] T. Alfrey, E.F. Gurnee, W.G. Lloyd, Diffusion in glassy polymers, J. Polym. Sci.: Part C 12 (1966) 249–261.
[2] G. Astarita, G.C. Sarti, A class of mathematical model for sorption of swelling solvent in glassy polymers, Polym. Eng. Sci. 18 (1978) 388–395.
[3] D. Andreucci, R. Ricci, A free boundary problem arising from sorption of solvents in glassy polymers, Quart. Appl. Math. XLIV (1987) 649–657.
[4] D.S. Cohen, Theoretical models for diffusion in glassy polymers, J. Polym. Sci.: Polym. Phys. Ed. 21 (1983) 2057–2065.
[5] D.S. Cohen, Theoretical models for diffusion in glassy polymers II, J. Polym. Sci.: Polym. Phys. Ed. 22 (1984) 1001–1009.
[6] D.S. Cohen, T. Erneux, Free boundary problems in controlled release pharmaceutical. I: diffusion in glassy polymers, SIAM J. Appl. Math. 48 (1988) 1451–1465.
[7] H.L. Frisch, Diffusion in glassy polymers II, J. Polym. Sci.: Part A-2 7 (1969) 879–887.
[8] N.L. Thomas, A.H. Windle, A theory of case II diffusion, Polymer 23 (1982) 529–542.
[9] P. Guidotti, Diffusion in glassy polymers: a free boundary value problem, Adv. Math. Sci. Appl. 7 (1997) 675–693.
[10] P. Guidotti, J.A. Pelesko, Transient instability in Case II diffusion, J. Polym. Sci.: Part B: Polym. Phys. 36 (1998) 2941–2947.
[11] T. Higuchi, Rate of release of medicaments from ointment bases containing drugs in suspension, J. Pharm. Sci. 50 (1961) 874–875.
[12] T. Higuchi, Mechanism of sustained-action medication, theoretical analysis of rate of release of drugs dispersed in solid matrices, J. Pharm. Sci. 52 (1963) 1145–1149.
[13] N.A. Peppas, R. Gurny, E. Doelker, P. Buri, Modelling of drug diffusion through swellable polymeric systems, J. Membr. Sci. 7 (1980) 241–253.
[14] J.S. Lin, C.C. Hwang, J.Y. Hsieh, Swelling controlled release of drug from polymeric delivery devices: a local similarity solution, J. Phys. Soc. Jpn. 69 (2000) 1991–1998.
[15] J.S. Lin, C.C. Hwang, C.M. Lin, J.Y. Lai, Solvent transport in spherical polymer-penetrant systems, Chem. Eng. Sci. 56 (2001) 151–156.